Translational perspectives on perfusion–diffusion mismatch in ischemic stroke

Bruce C. V. Campbell[1] and I. Mhairi Macrae[2]*

Magnetic resonance imaging has tremendous potential to illuminate ischemic stroke pathophysiology and guide rational treatment decisions. Clinical applications to date have been largely limited to trials. However, recent analyses of the major clinical studies have led to refinements in selection criteria and improved understanding of the potential implications for the risk vs. benefit of thrombolytic therapy. In parallel, preclinical studies have provided complementary information on the evolution of stroke that is difficult to obtain in humans due to the requirement for continuous or repeated imaging and pathological verification. We review the clinical and preclinical advances that have led to perfusion–diffusion mismatch being applied in phase 3 randomized trials and, potentially, future routine clinical practice.

Key words: diffusion imaging, MRI, penumbra, perfusion imaging, stroke, thrombolytic therapy

Magnetic Resonance Imaging (MRI) imaging of acute ischemic stroke in current clinical practice

Although a few centers now have MRI scanners in the emergency department or can access MRI rapidly for acute stroke patients, the clinical application of MRI for acute stroke treatment decision making has to date been fairly limited. The theoretical rationale for advanced imaging in acute ischemic stroke is to estimate the extent of potentially salvageable tissue in the 'penumbra' vs. the volume of 'ischemic core'. Penumbra is a concept defined in the 1970s (1) of hypoperfused and functionally impaired brain that can regain normal function if rapidly reperfused but otherwise has a high risk of progressing to infarction. Penumbra is the conceptual basis of all reperfusion therapies, and its existence is made possible by collateral flow via alternative blood flow routes, predominantly through the circle of Willis or leptomeningeal anastomoses (2). Ischemic core is defined as tissue that has been irreversibly damaged and will progress to infarction regardless of whether it is reperfused (3). Positron emission tomography (PET) has been used to identify these tissue states *in vivo* (4), and the hope for perfusion–diffusion MRI has been to provide more accessible estimates of ischemic core and penumbra in clinical practice.

Currently, the only proven reperfusion therapy is intravenous tissue plasminogen activator (tPA) administered within 4·5 h of stroke onset in patients selected using clinical criteria and noncontrast CT to exclude hemorrhage. Existing data using this approach suggest minimal benefit beyond 4·5 h (5). However, studies such as DEFUSE (6), EPITHET (7), and DEFUSE-2 (8) have demonstrated the potential for selecting patients who may benefit from reperfusion therapies beyond the current 4·5 h timeframe. The concept of perfusion–diffusion mismatch selection is now being tested in phase 3 trials such as EXTEND (9) and ECASS4-EXTEND. Some centers have been using extended time window MRI-based mismatch selection in clinical practice and have reported safety and clinical outcomes comparable with standard sub-4·5 h tPA patients in uncontrolled case series (10). This section of the review will address recent refinements in mismatch theory that are relevant to its clinical application.

Correspondence: I. Mhairi Macrae*, Institute of Neuroscience and Psychology, Wellcome Surgical Institute, University of Glasgow, Garscube Estate, Glasgow G61 1QH, UK.
E-mail: Mhairi.Macrae@glasgow.ac.uk
[1]Department of Medicine and Neurology, Melbourne Brain Centre at the Royal Melbourne Hospital, University of Melbourne, Victoria, Australia
[2]Institute of Neuroscience and Psychology, College of Medical, Veterinary and Life Sciences, University of Glasgow, Glasgow, UK

Conflicts of interest: B. C. V. Campbell received speaker's honoraria from Boehringer Ingelheim and acted as a consultant for Lundbeck. I. M. Macrae has nothing to declare.

DOI: 10.1111/ijs.12186

Diffusion imaging

Diffusion imaging is immensely powerful as a diagnostic tool in suspected stroke. It becomes abnormal within minutes of stroke onset (11) and has far greater sensitivity and specificity than any other current modality (12). Diffusion imaging is the key parameter to estimate irreversibly injured tissue in perfusion–diffusion mismatch or, for that matter, MRA-diffusion (13) or clinical-diffusion mismatch (14,15). The extent and location of the baseline diffusion lesion may be at least as important to clinical outcome after reperfusion as the volume of mismatch (16–18). Patients with large baseline diffusion-weighted imaging (DWI) lesions very rarely achieve a favorable clinical outcome, regardless of the success of reperfusion attempts. Indeed, these patients may be at greater risk of harm from reperfusion – the concept of 'malignant' or 'futile' profile (6). Current mismatch definitions include a maximum DWI lesion volume (e.g. <70 ml) in addition to the mismatch ratio and absolute volume of mismatch (8,9).

Considerable literature has evolved around the question of whether diffusion lesion reversal is a relevant clinical phenomenon (19). Much of this was confounded by inadequate attention to infarct atrophy, temporary postreperfusion reversal, and the milder spectrum of gliotic changes on follow-up Fluid Attenuated Inversion Recovery (FLAIR) imaging. Although the cytotoxic edema represented by diffusion restriction may be theoretically reversible (20), in clinical practice diffusion lesion reversal is rare. This has been studied predominantly beyond three-hours from onset when most stroke MRI is performed (21,22). One recent study that included 114 patients with pretreatment diffusion MR obtained <3 h from stroke onset found that 17% had reversal of >10 ml and >10% of the baseline lesion volume when reassessed at 24 h (23). Another similar sized but less quantitative study found predominantly temporary reversal in some cases on post-thrombolysis DWI with return of the lesion on FLAIR at seven-days (22). Temporary reversal is more common immediately after reperfusion,

although the time–course in humans is not well characterized (24). This is analogous to work in rats where 30 min of middle cerebral artery (MCA) occlusion lead to a diffusion lesion that completely vanished after reperfusion but later returned (25). In the same study, 10 min of MCA occlusion lead to a diffusion lesion that permanently disappeared. Histologically, however, there was neuronal loss indicating that the tissue salvage was incomplete. This incomplete tissue salvage in regions of normal FLAIR appearance, traditionally regarded as outside the infarct, has also been identified in man with reduced flumazenil binding using PET (26) and reduced magnetization transfer ratio using MRI (27). Thus, the common binary approach to defining irreversible injury using imaging, although pragmatic, is somewhat simplistic.

The best technique to measure diffusion lesion volume remains controversial. Single apparent diffusion coefficient (ADC) thresholds have been proposed but require significant postprocessing to achieve reasonable sensitivity while maintaining specificity as there is considerable overlap in the distribution of ADC values between injured and normal brain (28). The optimal ADC threshold may also vary with time from stroke onset (29). Although milder decreases in ADC are observed at the periphery of the lesion, these seem not to be salvaged in many cases, even with rapid reperfusion (24). For the purposes of automated segmentation, a combination of absolute ADC and relative B1000 intensity provides a reasonable approximation (30). However, for the greatest accuracy in research studies, we currently favor manual outlining of the 'maximal visual extent' of B1000 abnormality using careful windowing (24,31).

Perfusion imaging (PI) and the extent of ischemic penumbra

The survival of ischemic penumbra depends on the quality of collateral flow available to bypass an arterial occlusion. Collateral flow can occur via the circle of Willis or via leptomeningeal anastomoses between anterior cerebral artery (ACA), posterior cerebral artery (PCA) and the MCA. In laboratory animals, cerebral blood flow thresholds have been derived that have a time-dependent association with tissue viability (32). Studies using PET in a limited number of human patients with a variable degree of stroke acuity have suggested that similar relative thresholds, corresponding to a penumbra range of cerebral blood flow (CBF) ~17–22 ml/100 g/min, apply in man (33–35). Given the practical limitations of PET for clinical use, MRI dynamic susceptibility-weighted contrast PI has been applied.

Interestingly, delay-based parameters such as Tmax and TTP (time to peak of the deconvolved tissue residue function and raw concentration-time curve, respectively) have seemed more robust predictors of infarct risk than the relative CBF measures provided by MRI (36,37). Increased TTP and Tmax reflect the delay and dispersion incurred by flow travelling through collateral pathways. Simplistically, the longer the delay, the further the blood had to travel down the collateral vessels and the greater the risk of flow becoming inadequate to sustain tissue viability (38).

A key area of interest has been to distinguish tissue destined for infarction in the absence of reperfusion (one method of defining the 'ischemic penumbra') from that which will survive indefinitely even in the absence of reperfusion (so-called 'benign oligemia'). It has become clear that tissue experiencing mild degrees of perfusion delay (e.g. <4 s) at the periphery of the perfusion lesion almost never proceeds to infarction. Even with severe delays (e.g. Tmax >10 s) the risk of infarction without reperfusion is only around 70% (38). Multiple lines of evidence from PET correlation (37), xenon–CT correlation (39), and follow-up studies in patients without reperfusion (40,41) have suggested a delay of >4–6 s as the best threshold to define the tissue most likely to be at risk in an average patient (Fig. 1).

Precisely predicting the final infarct in an individual patient from a single snapshot of perfusion is probably impossible as stroke is a dynamic process with shifts in clot location and fluctuations in collateral flow (42). However, thresholding the perfusion lesion to exclude mild peripheral regions has been a significant advance in improving the relationship of mismatch volume with clinical response to reperfusion. A Tmax >6 s perfusion threshold was used in DEFUSE 2 (8), which confirmed the benefits of reperfusion in patients with mismatch beyond 4·5 h and is also employed in the ongoing EXTEND trial (9).

Defining mismatch

Early definitions of perfusion–diffusion mismatch used a mismatch ratio >1·2, which was an arbitrary choice based on the minimum visually evident difference in volume of two spheres. This criterion was combined with a minimum mismatch volume of 10 ml to avoid classifying 'mismatch' in very small lesions in the DEFUSE (6) and EPITHET (7) studies. Both studies used a generous definition of the perfusion lesion (Tmax ≥2 s), which lead to relatively high proportions of patients with mismatch (86% in EPITHET). Subsequent analyses emphasized the strong relationship of more stringent perfusion thresholds and/or higher mismatch ratios with improved response to reperfusion (41–44). As discussed above, the use of a Tmax >6 s threshold has been supported by PET and EPITHET–DEFUSE pooled sub-analyses. The recently published DEFUSE 2 study used a mismatch ratio >1·8, absolute mismatch volume >15 ml, and baseline DWI lesion volume <70 ml to define 'target mismatch' in patients about to undergo open label intra-arterial reperfusion therapy. Target mismatch patients had significantly better clinical and radiological outcomes if reperfusion was achieved compared with those in whom reperfusion therapy failed. The degree of reperfusion in these patients was directly related to the rate of good clinical outcome. In contrast, patients without target mismatch demonstrated no difference in outcome between reperfusion and non-reperfusion groups (8). The ongoing EXTEND randomized trial of tPA/placebo is using similar criteria (mismatch ratio >1·2, mismatch volume >10 ml, and DWI lesion volume <70 ml) to select patients 4·5–9 h after stroke onset or with wake-up onset stroke who may benefit from reperfusion (9). The importance of more selective mismatch definitions was recently highlighted in secondary analysis of the DIAS trial, which used visual assessment of perfusion–diffusion mismatch to select patients for thrombolysis with desmoteplase. This lead to the inclusion of many patients

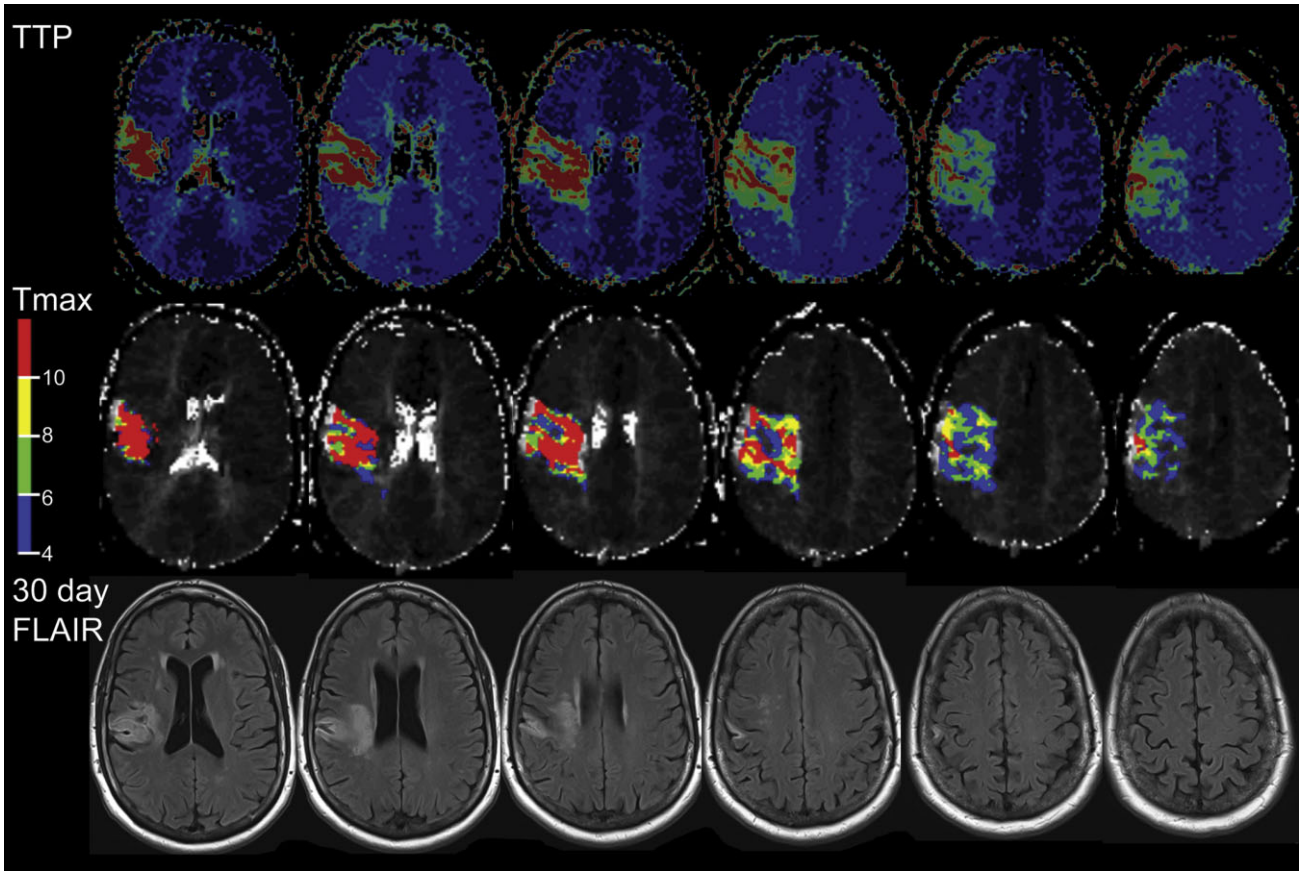

Fig. 1 Example of perfusion MRI in an acute ischemic stroke patient. Time to Peak (TTP) map generated by manufacturer's software demonstrates a clear abnormality in the right middle cerebral artery territory. However, without thresholding it is difficult to distinguish 'benign oligemia' from tissue at risk of infarction. The Tmax map (RAPID, Stanford University) quantifies the perfusion delay. Use of a Tmax >6 s threshold reduces the overestimation of tissue at risk, as seen when compared to the day 30 FLAIR in this patient who did not receive reperfusion therapy. MRI: Magnetic resonance imaging.

with small lesions, and the primary analysis was negative. However, reanalysis requiring mismatch of >60 ml demonstrated clear benefits of desmoteplase on clinical outcome (45).

An alternative approach to mismatch (46) was used in the recently published MR-RESCUE study (47). The investigators developed a complex multiparametric equation including DWI, ADC and several perfusion parameters to estimate the tissue likely to have already suffered irreversible injury at baseline. This method was based on the belief that DWI lesion reversal is an important issue. 'Mismatch' was defined using a volume of multiparametric-derived 'irreversible injury' <90 ml and <70% of perfusion lesion volume defined by Tmax >4 s. This selection approach did not lead to a positive trial result although the intra-arterial device intervention tested had limited efficacy in inducing recanalization and reperfusion. Patients with 'mismatch' did have better outcome in the presence of recanalization (assessed rather late at seven-days) but a similar trend was observed in nonmismatch patients, the reasons for which remain unclear (48).

Mismatch and vessel occlusion

Although mismatch can be considered in isolation, the 'dual target' combination of mismatch and major vessel occlusion has been proposed as a more powerful way to identify patients who will respond favorably to reperfusion. This is especially pertinent in trials, where power to detect a difference in good functional outcome with reperfusion may be greatest in patients with the severe baseline clinical deficits generally associated with major vessel occlusion. However, intravenous lytic agents are less effective in patients with major vessel occlusion, and this may counterbalance the benefits of dual target selection. Vessel occlusion is particularly relevant to intra-arterial clot retrieval therapies that are generally confined to the larger vessels. Mismatch has been argued to be less relevant in this context with the combination of vessel occlusion and small baseline DWI lesion proposed as simpler and equally useful in predicting response to therapy. In reality, the treatment decisions with either approach are usually concordant. However, mismatch is a more generalizable concept that may assist decision making when the baseline DWI lesion is moderately large and in patients without major vessel occlusion. Perfusion data may also provide extra information on treatment risk (49–52) and perhaps the probability of infarct expansion in the absence of reperfusion (38).

This review has not discussed CT perfusion, but this debate becomes irrelevant when CT is used as the same perfusion data are used to estimate both ischemic core and penumbra volumes and, in many cases, reconstruct dynamic angiography to assess vessel occlusion.

One significant pitfall of current mismatch approaches is that clinical response to reperfusion depends not only on the absolute mismatch volume but on the functional significance or 'eloquence' of the affected region. The dichotomous approach to mismatch, while necessary for clinical trials, is also somewhat arbitrary and masks a spectrum of pathophysiology. Incorporating qualitative spatial and functional information will be a key step in the translation of mismatch from enriching trial populations to guiding routine treatment for individual stroke patients. Ideally, the volume and functional role of the mismatch zone vs. the baseline DWI lesion would be weighed against an individualized assessment of hemorrhage risk.

MRI imaging of acute ischemic stroke: preclinical studies in rodents

Small animal MRI scanners, typically 7 tesla or higher magnetic field strength, are increasingly used to study the ischemic brain in animal stroke models [reviewed by Planas (53)]. Sequences used for routine clinical MRI, and more recent research techniques, have been set up on small animal scanners to facilitate 'bench to bedside' and 'bedside to bench' translational research. For example, T_2-weighted imaging for identification and quantitation of final infarct, DWI for acute ischemic injury, PI for perfusion deficit, diffusion tensor imaging for damage to white matter, T_1 imaging with contrast for blood brain barrier breakdown, and blood oxygen level dependent (BOLD) functional MRI for loss/return of function. As in clinical research, diffusion and PI are combined to generate PI/DWI mismatch for identification of potentially salvageable penumbral tissue.

There are both benefits and limitations associated with imaging stroke in animal models. One major benefit is the ability to track the evolution of damage and loss of penumbra by serially scanning over the first hours poststroke. Additionally, animals can undergo longitudinal study with multiple scanning sessions to track the consequences of a particular intervention over a number of weeks poststroke, and this can be combined with behavioral assessment of functional outcome. The major limitation is that during scanning, animals are anesthetized so that the head can be secured to limit movement. Therefore, the one important difference between clinical and preclinical stroke research is the need for anesthesia during stroke surgery and imaging. Anesthetics are known to influence blood pressure, respiration (and blood gases), cerebral blood flow, brain metabolism and function, and body temperature (54). Physiological monitoring and artificial respiration with regular blood gas analysis during prolonged scanning sessions (e.g. ≥6 h) enables physiology to be maintained within normal limits and the influence these parameters have on penumbra to be controlled.

Ischemic stroke models targeting the MCA have been established in a range of animals including gyrencephalic species such as the cat (55), miniature pig (56), and baboon (57). However, most imaging studies are carried out on rats, exposed to middle cerebral artery occlusion (MCAO). Imaging is also possible in mice (58) and is increasingly being used to phenotype transgenic mice (59–61).

Stroke is most commonly induced immediately prior to imaging but can be induced during the scanning session by occluding the MCA remotely (62,63). Penumbra is identified as tissue within the perfusion deficit, which has yet to show abnormality on diffusion scans (perfusion/diffusion mismatch). In the rodent stroke literature, ADC maps are generated from the diffusion data to obtain quantitative images of the diffusion coefficient. ADC and perfusion thresholds are then applied to define the borders of the diffusion abnormality and perfusion deficit, respectively. Relatively few groups have established ADC and perfusion thresholds (Table 1), with most rodent mismatch studies using one of these published thresholds (Table 2). However, it is important for groups to establish in-house thresholds specific to rat strain and time-point(s) being investigated as the ADC threshold has been shown to change with time from stroke onset (Li *et al.* (66), Table 1) and perfusion thresholds in one rat strain may not be applicable in other strains (Reid *et al.* (69), Table 1).

Data from published rodent mismatch studies are building up knowledge on the amount of penumbral tissue available for rescue in different rodent stroke models, including those with stroke-related comorbidity. A number of serial studies have also provided information on the evolution of damage and loss of penumbra in the acute period following stroke in the rat (Table 2).

Diffusion imaging and the acute diffusion lesion

Hyperintensity is already visible between 0 and 10 min after onset of ischemia on DWI scans when strokes are induced within the scanner. The intensity and size of the lesion gradually increases thereafter [0–6 h (62,63)]. The ADC threshold is calculated for a given time-point poststroke (usually three- to four-hours), with reference to the final (edema corrected) infarct size. For example, $0{\cdot}543 \times 10^{-3}$ mm^2/s or 83·5% of the contralateral hemisphere (excluding ventricles) at three-hour poststroke (65). In the studies that have derived in-house ADC thresholds, there is generally good agreement across strains and stroke models (Table 1). However, the rate of growth of the ADC-defined lesion is more variable and may depend on the strain of rat and the level of collateral supply to MCA territory, the size of the lesion on early scans, and the level of control of physiological variables (e.g. blood pressure, blood gases, and body temperature).

PI and the perfusion deficit

Most preclinical acute stroke imaging studies now employ arterial spin labeling (ASL), which does not require contrast agent injection and provides a direct assessment of CBF (Table 2) rather than the delay-based parameters, Tmax and TTP, used clinically. Perfusion deficits are defined using a similar threshold approach. A flow threshold is applied that represents the acute CBF or perfusion value that defines a tissue volume equal to final (edema corrected) infarct. The majority of studies that have defined a flow threshold have employed ASL (Table 1). Data are more variable

Table 1 Rat experimental stroke imaging papers where in-house perfusion and/or ADC thresholds were calculated

	Rat strain (n =) all male	Stroke model	Perfusion imaging	Perfusion threshold defined from:	Perfusion threshold (ml/100 g/min)	Contralateral/ normal CBF (ml/100 g/min)	ADC diffusion threshold defined from:	ADC threshold ($\times 10^{-3}$ mm^2/s)	Contralateral/normal ADC ($\times 10^{-3}$ mm^2/s)	Additional details	Reference
1	Wistar (6)	ILF	[^{14}C] iodoantipyrine autoradiography	Flow that matched tissue acidosis (pH <6·4)	31 ± 11		ADC value < control ADC minus 2 SD at two-hour poststroke	0·53 23% reduction (77% of control)	Cortex 0·726 ± 0·02 Caudate 0·659 ± 0·02 Mean = 0·6925	Threshold derived from single slice, 2·5 mm Mean ± SD	(64)
2	SD (9)	pMCAO + CCAO					ADC threshold value at one-hour poststroke that produced a lesion area = 24 h TTC infarct	Cortex 0·583 Caudate 0·501 Mean 0·542 14·5% reduction (85·5% of contra)	Cortex 0·678 Caudate 0·596	Thresholds derived from single 2 mm slice Mean ± SEM	(65)
							ADC threshold value at three-hour poststroke that produced a lesion area = 24 h TTC infarct	Cortex 0·587 Caudate 0·499 Mean 0·543 16·5% reduction (83·5% of contra)	Cortex 0·697 Caudate 0·609	Thresholds derived from single 2 mm slice Mean ± SEM	(65)
3	SD (13)	ILF					ADC threshold value at each time-point poststroke that produced a lesion volume = 24 h TTC infarct	25 min 0·62 (–16%) 60 min 0·60 (–18%) 90 min 0·54 (–24%) 150 min 0·52 (–28%) 210 min 0·50 (–30%) 270 min 0·5 (–30%)	0·67 ± 0·01	Thresholds derived from 6 × 2 mm slices Mean ± SD	(66)
4	SD (5)	ILF	ASL	CBF at 3 h poststroke that matched 24 h TTC edema-corrected infarct	30 ± 9 57 ± 11% reduction in flow	70 ± 30	ADC threshold value at three-hour poststroke that produced a lesion volume = 24 h TTC infarct	0·53 ± 0·03 30 ± 2% reduction	0·76 ± 0·03	Thresholds derived from 6 × 1·5 mm slices Mean ± SD	(67)
5	SD (5)	ILF	ASL	CBF at 3 h poststroke that matched 24 h TTC edema-corrected infarct	30 ± 9 57 ± 11% reduction in flow		ADC threshold value at three-hour poststroke that produced a lesion volume = 24 h TTC infarct	0·53 ± 0·03 30 ± 2% reduction		Thresholds derived from 6 × 1·5 mm slices Mean ± SD	(68)

Table 1 Continued

	Rat strain (n =) all male	Stroke model	Perfusion imaging	Perfusion threshold defined from:	Perfusion threshold (ml/100 g/min)	Contralateral/ normal CBF (ml/100 g/min)	ADC diffusion threshold defined from:	ADC threshold ($\times 10^{-3}$ mm^2/s)	Contralateral/normal ADC ($\times 10^{-3}$ mm^2/s)	Additional details	Reference
6	WKY (10)	ILF	ASL	CBF at 4 h poststroke that matched final edema-corrected infarct on T2-weighted scan	23 ± 8 81 ± 7% reduction in flow	124 ± 21	ADC threshold value at four-hour poststroke that produced a lesion volume = 24 h T2 edema-corrected infarct	0·61 ± 0·03 21 ± 4% reduction	0·76 ± 0·02	Thresholds derived from 6 × 1·5 mm slices Mean ± SD	(69)
7	SHRSP (10)	ILF	ASL	CBF at 4 h poststroke that matched final edema-corrected infarct on T2-weighted scan	36 ± 13 70 ± 9% reduction in flow	116 ± 13	ADC threshold value at four-hour poststroke that produced a lesion volume = 24 h T2 edema-corrected infarct	0·59 ± 0·03 23 ± 4% reduction	0·76 ± 0·01	Thresholds derived from 6 × 1·5 mm slices Mean ± SD	(69)
8	SD (9)	ILF	ASL	Mean minus 2 SD of prestroke ipsi hemisphere	72 ± 14% reduction in flow	220–300	Mean ADC of prestroke ipsi hemisphere minus 2 SD	33 ± 7% reduction	0·74 ± 0·06	Pixel by pixel analysis used to generate penumbra volume Mean ± SD	(70)
9	WKY (10) SHR (11) RH-WKY (10)	ILF	Bolus iv Magnevist	TTP > contralateral tissue <2 SD of basal signal drop <3 SD of basal signal			Mean contralateral ADC (excluding ventricles) minus 2 SD	0·6 26% reduction	0·810 ± 0·11	Thresholds derived from 7 × 1·5 mm slices with 0·5 mm interslice gap Mean ± SEM	(71)

ADC, apparent diffusion coefficient; ASL, arterial spin labeling; CBF, cerebral blood flow; contra, contralateral hemisphere; ILF, intraluminal filament; pMCAO + CCAO, proximal diathermy-induced permanent MCAO + common carotid artery occlusion; RH-WKY, renovascular-hypertensive Wistar Kyoto rat; SD, Sprague Dawley rat; SHR, spontaneously hypertensive rat; SHRSP, spontaneously hypertensive stroke prone rat; WKY, Wistar Kyoto rat.

Table 2 Selection of rat stroke imaging papers where mismatch volumes are presented

	Rat strain (*n* =), all male	Stroke model	Time mismatch was assessed poststroke (min)	Approx mismatch size mm^3	Source of ADC thresholds used	Source of Perfusion threshold used	Additional details	Reference
1	SD (11)	ILF	30 60 90 120 180	SD ~60 SD ~22 SD ~22 SD ~17 SD ~10	Shen *et al.* (67)	Shen *et al.* (67)	Four, 1·5-mm slices analyzed using Matlab voxel-based analysis	(67)
2	SD (9) WKY (9)	ILF	45 90 120 180 210	SD ~89 WKY ~116 SD ~33 WKY ~75 SD ~12 WKY ~52 SD ~4 WKY ~35 SD ~4 WKY ~26	Meng *et al.* (68)	Meng *et al.* (68)	Eight, 1·5-mm slices analyzed using Matlab voxel-based analysis & STIMULATE	(72)
3	SD (6)	ILF	106	SD 22	Lo *et al.* (65)	Meng *et al.* (68)	Two, 1·5 mm slices within MCA territory	(73)
4	SD (8)	ILF	72	SD 20	Lo *et al.* (65)	Meng *et al.* (68)	Two, 1·5 mm slices within MCA territory	(74)
5	SD (9)	ILF	60 120 180 240	SD ~154 µl SD ~185 µl SD ~144 µl SD ~165 µl	Foley *et al.* (70)	Foley *et al.* (70)	Matlab voxel-based analysis PaO_2 run at 235–240 mmHg	(70)
6	Wistar (4)	ILF	25 45 60 90 120 150 180	Wistar ~85 Wistar ~70 Wistar ~52 Wistar ~37 Wistar ~20 Wistar ~20 Wistar ~14	Meng *et al.* (68)	Meng *et al.* (68)	Seven, 1·5 mm slices analyzed with QuickVol II	(75)
7	Wistar (8)	ILT	25 45 70 90 120 150 180	Wistar ~64 Wistar ~62 Wistar ~44 Wistar ~26 Wistar ~18 Wistar ~20 Wistar ~12	Meng *et al.* (68)	Meng *et al.* (68)	Images were analyzed using QuickVol II as detailed by Meng *et al.* (68)	(76)
8	SD (11)	ILF	30 60 90 120 180	SD ~81 SD ~33 SD ~28 SD ~20 SD ~4	Meng *et al.* (68)	Meng *et al.* (68)	Mismatch volume was perfusion deficit volume minus ADC lesion volume calculated from pixels within abnormal areas on ADC & CBF maps that were identified using in-house thresholds on six 1·5 mm slices	(68)
9	WKY (12) SHRSP (15)	ILF	60 120 180 240	WKY 43 SHRSP 34 WKY 32 SHRSP 37 WKY 27 SHRSP 32 WKY 29 SHRSP 23	Reid *et al.* (69) (WKY) Reid *et al.* (69) (SHRSP)	Reid *et al.* (69) (WKY) Reid *et al.* (69) (SHRSP)	Six 1·5 mm slices analyzed using Matlab voxel-based analysis	(69)
10	WKY (9) RH-WKY (7) SHR (11)	ILF	30 90 120 150 240	WKY 117 RH-WKY 55 SHR 66 WKY 93 RH-WKY 34 SHR 24 WKY ~89 RH-WKY ~12 SHR ~17 WKY ~87 RH-WKY ~15 SHR ~10 WKY ~50 RH-WKY ~15 SHR ~4	Letourneur *et al.* (71)	Letourneur *et al.* (71)	Seven 1·5 mm slices with a 0·5 mm interslice gap. Mismatch volume was perfusion deficit volume minus ADC lesion volume	(71)

All studies involved permanent MCAO using the intraluminal filament model. Mismatch volumes are approximate (~) as they were manually estimated from published figures. ADC, apparent diffusion coefficient; ILF, intraluminal filament; RH-WKY, renovascular-hypertensive rat; SD, Sprague Dawley rat; SHR, spontaneously hypertensive rat; SHRSP, spontaneously hypertensive stroke prone rat; WKY, Wistar Kyoto rat.

than for ADC values (e.g. see range of contralateral CBF values, Table 1) and consequently there is a wider spread in published flow thresholds.

In the majority of rodent studies, the volume of perfusion deficit remains relatively constant over the first four- to six-hours following stroke, with reductions in the mismatch volume reflecting increases in the volume of the ADC lesion (68,72,75,76). However, in some studies, the perfusion deficit also increases over time (69,70,77), which could point to a failure of collateral flow. These studies used spontaneously hypertensive stroke-prone, Wistar Kyoto and Sprague Dawley rats. In situations where the perfusion deficit and DWI lesion grow at a similar rate, this could give the false impression of survival of penumbral tissue as overall mismatch volume would not change with time.

Penumbra and perfusion/diffusion mismatch

Preclinically, penumbra volume can be assessed using at least three different methods:

- by simply subtracting the ADC-derived lesion volume from the perfusion deficit volume at each time-point (volumetric perfusion–diffusion mismatch with no anatomical coregistration, most common);
- slice-by-slice delineation of ADC-derived lesion, perfusion deficit, and mismatch area using coregistration software (e.g. Image J, U. S. National Institutes of Health, Bethesda, Maryland, USA) or voxel-based analysis (e.g. Matlab Mathworks, Natick, Massachusetts, USA); and
- retrospective assessment of penumbra by subtracting the ADC lesion volume at a given time-point from the final edema-corrected infarct.

The size and location of penumbra varies according to the thresholds applied and also which of the three approaches is employed (69). All published studies using these methods have detected a measureable mismatch volume at early time-points, within the range presented in Table 2 and which generally reduces in size over time. Mismatch volume and its rate of loss vary across different normotensive rat strains (Table 2), with studies on rats with comorbidity (e.g. hypertension) reporting smaller mismatch volumes (69,71,77). Therefore, available techniques provide the means to quantify how much penumbral tissue is available for tissue salvage and to investigate the potential for therapies to save or extend penumbra life span. However, direct comparison of mismatch volume between studies is hampered by a lack of standardization in the rostro-caudal extent of MCA territory covered by the scans (see Table 2).

Type and depth of anesthesia can influence the temporal change in the ADC lesion and perfusion deficit and therefore the assessment of penumbra from DWI/PI or ADC/PI mismatch. Instances can arise preclinically where mismatch volume is maintained (e.g. over a period of four-hours or longer) without intervention. For example, where the ADC lesion volume does not increase with time (possibly due to tight control of physiological variables under anesthesia and/or enhanced oxygenation of ventilation gases), or when the size of the perfusion deficit increases at a similar rate to ADC lesion growth. In permanent MCAO models, the volume of hypoperfused tissue, detected acutely, can exceed the final (edema corrected) infarct at 24 h, making threshold setting problematic. One explanation for this may be that the increase in blood pressure, on withdrawal of anesthesia, causes an increase in CBF within the ischemic hemisphere such that the volume of perfusion deficit is reduced and, consequently, more tissue survives. Therefore, the potential for anesthesia to influence penumbra size is not inconsiderable and should be taken into account when interpreting results.

Summary

A number of preclinical centers are now equipped for rodent MRI research on the ischemic penumbra. What is needed now is for a consensus to be reached and the optimum protocols for generating and processing mismatch data standardized across all centers. Then preclinical MRI will provide a powerful platform to research the penumbra and test novel therapeutic strategies for tissue salvage or to prolong its life span, which hopefully will translate to the clinic. Physiological stability under anesthesia will be key to interpretation of results and reproducibility of findings across sites. Clinical application of perfusion–diffusion mismatch has already entered practice in some centers. However, studies thus far have had mixed success in demonstrating treatment effects in patients selected using various mismatch paradigms. As with preclinical work, much has been learned from these experiences about the importance of thresholding perfusion lesions and standardizing processing and interpretation. The current generation of clinical trials in progress provides hope for a future in which patient treatment can be individualized on the basis of pathophysiology, illuminated by imaging.

References

1 Astrup J, Siesjö BK, Symon L. Thresholds in cerebral ischemia – the ischemic penumbra. *Stroke* 1981; **12:**723–5.
2 Shuaib A, Butcher K, Mohammad AA, Saqqur M, Liebeskind DS. Collateral blood vessels in acute ischaemic stroke: a potential therapeutic target. *Lancet Neurol* 2011; **10:**909–21.
3 Wintermark M, Albers GW, Broderick JP *et al.*; for the Stroke Imaging Research (STIR) and VISTA-Imaging Investigators. Acute Stroke Imaging Research Roadmap II. *Stroke* 2013; doi: 10.1161/STROKEAHA.113.002015.
4 Heiss W-D. Ischemic penumbra: evidence from functional imaging in man. *J Cereb Blood Flow Metab* 2000; **20:**1276–93.
5 Lees KR, Bluhmki E, von Kummer R *et al.* Time to treatment with intravenous alteplase and outcome in stroke: an updated pooled analysis of ECASS, ATLANTIS, NINDS, and EPITHET trials. *Lancet* 2010; **375:**1695–703.
6 Albers GW, Thijs VN, Wechsler L *et al.* Magnetic resonance imaging profiles predict clinical response to early reperfusion: the diffusion and perfusion imaging evaluation for understanding stroke evolution (DEFUSE) study. *Ann Neurol* 2006; **60:**508–17.
7 Davis SM, Donnan GA, Parsons MW *et al.* Effects of alteplase beyond 3 h after stroke in the Echoplanar Imaging Thrombolytic Evaluation Trial (EPITHET): a placebo-controlled randomised trial. *Lancet Neurol* 2008; **7:**299–309.
8 Lansberg MG, Straka M, Kemp S *et al.* MRI profile and response to endovascular reperfusion after stroke (DEFUSE 2): a prospective cohort study. *Lancet Neurol* 2012; **11:**860–7.
9 Ma H, Parsons MW, Christensen S *et al.* A multicentre, randomized, double blinded, placebo controlled phase 3 study to investigate

EXtending the time for Thrombolysis in Emergency Neurological Deficits (EXTEND). *Int J Stroke* 2012; **7:**74–80.
10 Schellinger PD, Thomalla G, Fiehler J *et al.* MRI-based and CT-based thrombolytic therapy in acute stroke within and beyond established time windows: an analysis of 1210 patients. *Stroke* 2007; **38:**2640–5.
11 Hjort N, Christensen S, Sølling C *et al.* Ischemic injury detected by diffusion imaging 11 minutes after stroke. *Ann Neurol* 2005; **58:** 462–5.
12 Schellinger PD, Bryan RN, Caplan LR *et al.* Evidence-based guideline: the role of diffusion and perfusion MRI for the diagnosis of acute ischemic stroke: report of the Therapeutics and Technology Assessment Subcommittee of the American Academy of Neurology. *Neurology* 2010; **75:**177–85.
13 Lansberg MG, Thijs VN, Bammer R *et al.* The MRA-DWI mismatch identifies patients with stroke who are likely to benefit from reperfusion. *Stroke* 2008; **39:**2491–6.
14 Davalos A, Blanco M, Pedraza S *et al.* The clinical-DWI mismatch: a new diagnostic approach to the brain tissue at risk of infarction. *Neurology* 2004; **62:**2187–92.
15 Lansberg MG, Thijs VN, Hamilton S *et al.* Evaluation of the clinical-diffusion and perfusion-diffusion mismatch models in DEFUSE. *Stroke* 2007; **38:**1826–30.
16 Parsons MW, Christensen S, McElduff P *et al.* Pretreatment diffusion- and perfusion-MR lesion volumes have a crucial influence on clinical response to stroke thrombolysis. *J Cereb Blood Flow Metab* 2010; **30:**1214–25.
17 Yoo AJ, Verduzco LA, Schaefer PW *et al.* MRI-based selection for intra-arterial stroke therapy: value of pretreatment diffusion-weighted imaging lesion volume in selecting patients with acute stroke who will benefit from early recanalization. *Stroke* 2009; **40:**2046–54.
18 Menezes NM, Ay H, Wang Zhu M *et al.* The real estate factor: quantifying the impact of infarct location on stroke severity. *Stroke* 2007; **38:**194–7.
19 Kranz PG, Eastwood JD. Does diffusion-weighted imaging represent the ischemic core? An evidence-based systematic review. *AJNR Am J Neuroradiol* 2009; **30:**1206–12.
20 Simard JM, Kent TA, Chen M, Tarasov KV, Gerzanich V. Brain oedema in focal ischaemia: molecular pathophysiology and theoretical implications. *Lancet Neurol* 2007; **6:**258–68.
21 Chemmanam T, Campbell BC, Christensen S *et al.* Ischemic diffusion lesion reversal is uncommon and rarely alters perfusion-diffusion mismatch. *Neurology* 2010; **75:**1040–7.
22 Sakamoto Y, Kimura K, Shibazaki K *et al.* Early ischaemic diffusion lesion reduction in patients treated with intravenous tissue plasminogen activator: infrequent, but significantly associated with recanalization. *Int J Stroke* 2013; **8:**321–6.
23 Labeyrie MA, Turc G, Hess A *et al.* Diffusion lesion reversal after thrombolysis: a MR correlate of early neurological improvement. *Stroke* 2012; **43:**2986–91.
24 Campbell BCV, Purushotham A, Christensen S *et al.* The infarct core is well represented by the acute diffusion lesion: sustained reversal is infrequent. *J Cereb Blood Flow Metab* 2012; **32:**50–6.
25 Li F, Liu KF, Silva MD *et al.* Transient and permanent resolution of ischemic lesions on diffusion-weighted imaging after brief periods of focal ischemia in rats: correlation with histopathology. *Stroke* 2000; **31:**946–54.
26 Guadagno JV, Jones PS, Aigbirhio FI *et al.* Selective neuronal loss in rescued penumbra relates to initial hypoperfusion. *Brain* 2008; **131:**2666–78.
27 Tourdias T, Dousset V, Sibon I *et al.* Magnetization transfer imaging shows tissue abnormalities in the reversible penumbra. *Stroke* 2007; **38:**3165–71.
28 Purushotham A, Campbell BC, Straka M *et al.* Apparent diffusion coefficient threshold for delineation of ischemic core. *Int J Stroke* 2013, doi: 10.1111/ijs.12068.
29 An H, Ford AL, Vo K, Powers WJ, Lee JM, Lin W. Signal evolution and infarction risk for apparent diffusion coefficient lesions in acute ischemic stroke are both time- and perfusion-dependent. *Stroke* 2011; **42:**1276–81.
30 Straka M, Albers GW, Bammer R. Real-time diffusion-perfusion mismatch analysis in acute stroke. *J Magn Reson Imaging* 2010; **32:**1024–37.
31 Butcher K, Parsons M, Allport L *et al.* Rapid assessment of perfusion-diffusion mismatch. *Stroke* 2008; **39:**75–81.
32 Jones TH, Morawetz RB, Crowell RM *et al.* Thresholds of focal cerebral ischemia in awake monkeys. *J Neurosurg* 1981; **54:**773–82.
33 Marchal G, Beaudouin V, Rioux P *et al.* Prolonged persistence of substantial volumes of potentially viable brain tissue after stroke: a correlative PET-CT study with voxel-based data analysis. *Stroke* 1996; **27:**599–606.
34 Hakim AM, Evans AC, Berger L *et al.* The effect of nimodipine on the evolution of human cerebral infarction studied by PET. *J Cereb Blood Flow Metab* 1989; **9:**523–34.
35 Baron JC. Perfusion thresholds in human cerebral ischemia: historical perspective and therapeutic implications. *Cerebrovasc Dis* 2001; **11**(Suppl. 1)**:**2–8.
36 Christensen S, Mouridsen K, Wu O *et al.* Comparison of 10 perfusion MRI parameters in 97 sub-6-hour stroke patients using voxel-based receiver operating characteristics analysis. *Stroke* 2009; **40:**2055–61.
37 Zaro-Weber O, Moeller-Hartmann W, Heiss WD, Sobesky J. Maps of time to maximum and time to peak for mismatch definition in clinical stroke studies validated with positron emission tomography. *Stroke* 2010; **41:**2817–21.
38 Nagakane Y, Christensen S, Ogata T *et al.* Moving beyond a single perfusion threshold to define penumbra: a novel probabilistic mismatch definition. *Stroke* 2012; **43:**1548–55.
39 Olivot JM, Mlynash M, Zaharchuk G *et al.* Perfusion MRI (Tmax and MTT) correlation with xenon CT cerebral blood flow in stroke patients. *Neurology* 2009; **72:**1140–5.
40 Christensen S, Campbell BCV, Perez de la Ossa N *et al.* Optimal perfusion thresholds for prediction of tissue destined for infarction in the combined EPITHET and DEFUSE dataset. *Stroke* 2010; **41:**e297.
41 Olivot JM, Mlynash M, Thijs VN *et al.* Optimal Tmax threshold for predicting penumbral tissue in acute stroke. *Stroke* 2009; **40:**469–75.
42 Campbell BCV, Christensen S, Tress BM *et al.* Failure of collateral blood flow is associated with infarct growth in ischemic stroke. *J. Cereb Blood Flow and Metab* 2013; **33:**1168–72.
43 Christensen S, Parsons MW, De Silva DA *et al.* Optimal mismatch definitions for detecting treatment response in acute stroke. *Cerebrovasc Dis* 2008; **25**(Suppl. 2)**:**33.
44 Kakuda W, Lansberg MG, Thijs VN *et al.* Optimal definition for PWI/DWI mismatch in acute ischemic stroke patients. *J Cereb Blood Flow Metab* 2008; **28:**887–91.
45 Warach S, Al-Rawi Y, Furlan AJ *et al.* Refinement of the magnetic resonance diffusion-perfusion mismatch concept for thrombolytic patient selection: insights from the desmoteplase in acute stroke trials. *Stroke* 2012; **43:**2313–8.
46 Kidwell CS, Wintermark M, De Silva DA *et al.* Multiparametric MRI and CT models of infarct core and favorable penumbral imaging patterns in acute ischemic stroke. *Stroke* 2013; **44:**73–9.
47 Kidwell CS, Jahan R, Gornbein J *et al.* A trial of imaging selection and endovascular treatment for ischemic stroke. *N Engl J Med* 2013; **368:**914–23.
48 Parsons MW, Albers GW. MR RESCUE: is the glass half-full or half-empty? *Stroke* 2013; **44:**2055–7.
49 Campbell BCV, Christensen S, Parsons MW *et al.* Advanced imaging improves prediction of hemorrhage after stroke thrombolysis. *Ann Neurol* 2013; **73:**510–19.
50 Campbell BCV, Christensen S, Butcher KS *et al.* Regional very low cerebral blood volume predicts hemorrhagic transformation better than diffusion-weighted imaging volume and thresholded apparent diffusion coefficient in acute ischemic stroke. *Stroke* 2010; **41:**82–8.
51 Kim JH, Bang OY, Liebeskind DS *et al.* Impact of baseline tissue status (diffusion-weighted imaging lesion) versus perfusion status (severity

of hypoperfusion) on hemorrhagic transformation. *Stroke* 2010; **41:**e135–42.
52 Mlynash M, Lansberg MG, De Silva DA *et al*. Refining the definition of the malignant profile: insights from the DEFUSE-EPITHET pooled data set. *Stroke* 2011; **42:**1270–5.
53 Planas AM. Noninvasive brain imaging in small animal stroke models: MRI and PET; in Dirnagl U (ed.): Rodent Models of Stroke. Springer Protocols Neuromethods 47. New York, Humana Press, 2010**:**139–65.
54 Traystman RJ. Effect of anaesthesia in stroke models; in Dirnagl U (ed.): Rodent Models of Stroke. Springer Protocols Neuromethods 47. New York, Humana Press, 2010**:**121–38.
55 Bulloch R, McCulloch J, Graham DI, Lowe D, Chen MH, Teasdale GM. Focal ischemia in the cat: pre-treatment with a competitive NMDA receptor antagonist, D-CPP-ene. *J Cereb Blood Flow Metab* 1990; **10:**668–74.
56 Imai H, Konno K, Nakamura M *et al*. A new model of focal cerebral ischaemia in the miniature pig. *J Neurosurg* 2006; **104:**123–32.
57 Yonas H, Wolfson SK, Dujovny M, Boehnke M, Cook E. Selective lenticulostriate occlusion in the primate. A highly focal cerebral ischemia model. *Stroke* 1981; **12:**567–72.
58 Hesselbarth D, Franke C, Hata R, Brinker G, Hoehn-Berlage M. High resolution MRI and MRS: a feasibility study for the investigation of focal cerebral ischemia in mice. *NMR Biomed* 1998; **11:**423–9.
59 Paul R, Zhang ZG, Eliceiri BP *et al*. Src deficiency or blockade of Src activity in mice provides cerebral protection following stroke. *Nat Med* 2001; **7:**222–7.
60 Hughes PM, Allegrini PR, Rudin M, Perry VH, Mir AK, Wiessner C. Monocyte chemoattractant protein-1 deficiency is protective in a murine stroke model. *J Cereb Blood Flow Metab* 2002; **22:**308–17.
61 Anderson SA, Frank JA. MRI of mouse models of neurological disorders. *NMR Biomed* 2007; **20:**200–15.
62 Hoehn-Berlage M, Hossmann KA, Busch E, Eis M, Schmitz B, Gyngell ML. Inhibition of nonselective cation channels reduces focal ischemic injury of rat brain. *J Cereb Blood Flow Metab* 1997; **17:**534–42.
63 Li F, Han S, Tatlisumak T *et al*. A new method to improve in-bore middle cerebral artery occlusion in rats: demonstration with diffusion- and perfusion-weighted imaging. *Stroke* 1998; **29:**1715–20.
64 Hoehn-Berlage M, Norris DG, Kohno K, Mies G, Leibfritz D, Hossmann K-A. Evolution of regional changes in apparent diffusion coefficient during focal ischemia of rat brain: the relationship of quantitative diffusion NMR imaging to reduction in cerebral blood flow and metabolic disturbance. *J Cereb Blood Flow Metab* 1995; **5:**1002–11.
65 Lo EH, Pierce AR, Mandeville JB, Rosen BR. Neuroprotection with NBQX in rat focal cerebral ischemia. Effects on ADC probability distribution functions and diffusion–perfusion relationships. *Stroke* 1997; **28:**439–47.
66 Li F, Carano RAD, Irie K, Sotak CH, Fisher M. Temporal evolution of average apparent diffusion coefficient threshold to define ischemic abnormalities in a rat permanent occlusion model. *J Stroke Cerebrovasc Dis* 2000; **9:**1–7.
67 Shen Q, Meng X, Fisher M, Sotak CH, Duong TQ. Pixel-by-pixel spatiotemporal progression of focal ischemia derived using quantitative perfusion and diffusion imaging. *J Cereb Blood Flow Metab* 2003; **23:**1479–88.
68 Meng X, Fisher M, Shen Q, Sotak CH, Duong TQ. Characterizing the diffusion/perfusion mismatch in experimental focal cerebral ischemia. *Ann Neurol* 2004; **55:**207–12.
69 Reid E, Graham D, Lopez-Gonzalez MR, Holmes WM, Macrae IM, McCabe C. Penumbra detection using PWI/DWI mismatch MRI in a rat stroke model with and without co-morbidity: comparison of methods. *J Cereb Blood Flow Metab* 2012; **32:**1765–77.
70 Foley LM, Hitchens TK, Barbe B *et al*. Quantitative temporal profiles of penumbra and infarction during permanent middle cerebral artery occlusion in rats. *Transl Stroke Res* 2010; **1:**220–9.
71 Letourneur A, Roussel S, Toutain J, Bernaudin M, Touzani O. Impact of genetic and renovascular chronic arterial hypertension on the acute spatiotemporal evolution of the ischemic penumbra: a sequential study with MRI in the rat. *J Cereb Blood Flow Metab* 2011; **31:**504–13.
72 Bardutzky J, Shen Q, Henninger N, Bouley J, Duong TQ, Fisher M. Differences in ischemic lesion evolution in different rat strains using diffusion and perfusion imaging. *Stroke* 2005; **36:**2000–5.
73 Robertson C, McCabe C, Gallagher L *et al*. Stroke penumbra defined by an MRI-based oxygen challenge technique: 1. Validation using [^{14}C]2-deoxyglucose autoradiography. *J Cereb Blood Flow Metab* 2011; **31:**1778–87.
74 Robertson C, McCabe C, Gallagher L *et al*. Stroke penumbra defined by an MRI-based oxygen challenge technique: 2. Validation based on the consequences of reperfusion. *J Cereb Blood Flow Metab* 2011; **31:**1788–98.
75 Bråtane BT, Bouley J, Schneider A, Bastan B, Henninger N, Fisher M. Granulocyte-colony stimulating factor delays PWI/DWI mismatch evolution and reduces final infarct volume in permanent-suture and embolic focal cerebral ischemia models in the rat. *Stroke* 2009; **40:**3102–6.
76 Bråtane BT, Cui H, Cook DJ, Bouley J, Tymianski M, Fisher M. Neuroprotection by freezing ischemic penumbra evolution without cerebral blood flow augmentation with a postsynaptic density-95 protein inhibitor. *Stroke* 2011; **42:**3265–70.
77 McCabe C, Gallagher L, Gsell W, Graham D, Dominiczak AF, Macrae IM. Differences in the evolution of the ischaemic penumbra in the SHRSP and WKY rat. *Stroke* 2009; **40:**3864–8.